

Are modified pumpkin flour/plum flour nanocomposite films biodegradable and compostable?



Tomy J. Gutiérrez

Grupo de Materiales Compuestos Termoplásticos (CoMP), Instituto de Investigaciones en Ciencia y Tecnología de Materiales (INTEMA), Facultad de Ingeniería, Universidad Nacional de Mar del Plata (UNMDP) y Consejo Nacional de Investigaciones Científicas y Técnicas (CONICET), Colón 10850, B7608FLC, Mar del Plata, Argentina

ARTICLE INFO

Keywords:

Food packaging
Structure
Surface
Thermal behavior
Thermoplastic flour

ABSTRACT

Nanocomposite films made from nonconventional food hydrocolloids: phosphated or methylated flours derived from pumpkin (*Cucurbita maxima*) with or without “huesito” plum (*Spondias purpurea*) flour, were obtained by the casting methodology. The films were characterized, and in addition two biomarkers of ecotoxicity, survival and weight changes, were determined for each one by means of a novel bioassay using the furniture weevil (*Tricorynus sp.*, Coleoptera: Anobiidae). The films prepared from the methylated flours had a lower sensitivity to water, greater thermal resistance and higher crystallinity percentage than the phosphated flour films. However, these materials were very fragile, as well as being ecotoxic, thus limiting their compostability. Thus, although both the phosphated and methylated pumpkin flour-based films were biodegradable only the phosphated films can be considered as eco-friendly. The plum flour nanocomposite was included due to the anthocyanins it contains, with the aim of developing pH-sensitive films. Unfortunately, neither of the resulting nanocomposite films achieved this objective. Nevertheless, their mechanical and thermal properties were improved, and the ecotoxicity levels reduced, compared to the films prepared without the nanocomposite.

1. Introduction

The development and manufacture of food packaging (films and coatings) derived from hydrocolloids (starch, proteins, and gums) has boomed over the last three decades, as packaging made from these materials can extend food shelf-life, as well as providing a solution to the pollution caused by synthetic polymer-based packaging materials (Álvarez, Alvarez, & Gutiérrez, 2018). In recent years, flours in particular have attracted much attention as food packaging materials as they have biopolymer matrices that produce films with better physico-chemical properties than those prepared from isolated starch or proteins (Pelissari, Andrade-Mahecha, Sobral, & Menegalli, 2013). This is mainly due to the chemical interactions that take place between the components of the flours (Gutiérrez & Álvarez, 2016). In addition, flour offers a higher yield compared to starch (Gutiérrez & Alvarez, 2017a). Flours as polymer matrices for the development of films also share some of the favorable characteristics of starch: they are economical, abundant, easy to obtain, renewable, and innocuous (Otoni et al., 2017). In this study, we propose the manufacture and use of pumpkin flour (*Cucurbita maxima*) as an unconventional biopolymer matrix for the development of films. According to the published literature only films based on pumpkin oil cake, a by-product obtained after extracting oil from pumpkin seed (*Cucurbita pepo* L.) by cold-pressing, have been

manufactured, but there is no record of the use of pumpkin flour for film development (Popović, Peričin, Vaštag, Lazić, & Popović, 2012; Popović, Peričin, Vaštag, Popović, & Lazić, 2011).

According to the Food and Agriculture Organization of the United Nations (FAO, 2014) the world production of pumpkins occurs over an area of 1,775,000 hectares, with a production of 24.3 million tons/year. Since the year 2000 there has been an increase in production of 36.5%, from 17.8 to 24.3 million tons/year, with 48% undertaken by only two countries, China (28.7%) and India (19.3%). Argentina ranks among the top 10 producing countries, with an estimated production volume of between 420,000 and 450,000 tons in an area close to 25,000 hectares. Although this crop is developed throughout the whole of Argentina, Buenos Aires, Mendoza and Santiago del Estero are the main producing provinces. The FAO (2014) report also highlighted that more than 85% of total imports worldwide are absorbed by only seven countries, notably the United States with 41%. As for the main exporting countries, more than 90% of the total is undertaken by eight countries, led by Spain with 42.68%.

In spite of the aforementioned advantages of biopolymer-based films, their susceptibility to moisture and tendency towards brittleness are challenges that still need to be overcome (Gutiérrez, González Seligra, Medina Jaramillo, Famá, & Goyanes, 2017). In order to achieve this, several studies have produced modified flour biopolymer matrices

E-mail address: tomy.gutierrez@fi.mdp.edu.ar.

<https://doi.org/10.1016/j.foodhyd.2018.05.035>

Received 29 January 2018; Received in revised form 16 May 2018; Accepted 16 May 2018

Available online 21 May 2018

0268-005X/ © 2018 Elsevier Ltd. All rights reserved.

to which composites are also added. As regards the composites, these are preferably in the nanometric size range, since this enables a stronger interaction with the matrix, resulting in materials that are less sensitive to humidity and more resistant (Bracone, Merino, González, Alvarez, & Gutiérrez, 2016). In this study, phosphorylation and methylation were performed to modify the polymer matrix. Phosphorylation has been shown to result in the development of less hydrophilic materials by 1) reducing the number of hydroxyl groups (polar sites) within the structure of the starch via the crosslinking reaction, and 2) increasing glycerol-phosphated starch interactions within the starch structure by the introduction of phosphate groups, which compensates for the polar sites within the matrix (Gutiérrez, Morales, Pérez, Tapia, & Famá, 2015). Methylation, on the other hand, reduces the moisture susceptibility of films due to the occurrence of a second-order aliphatic electrophilic substitution reaction (SN2) which replaces the hydroxyl groups in the starch structure by apolar groups such as methyl ($-\text{CH}_3$) (Sívoli et al., 2013).

The nanocomposite employed in this study was derived from “huesito” plum (*Spondias purpurea*) peel, and was included as a natural reinforcement material within the polymer matrices. The reasons for using plum peel to develop the nanocomposite were that 1) cellulosic materials are widely used as reinforcement materials in both natural and synthetic polymers, and the peel of the fruits is where the highest fiber content in the form of cellulose is found (Gutiérrez & Alvarez, 2017b), and 2) high concentrations of anthocyanins have been found in the peel of “huesito” plums (Ferreira de Almeida et al., 2017; Muñoz-López, Urrea-García, Jiménez-Fernández, Rodríguez-Jiménez, & Luna-Solano, 2018). Research done over the last five years has shown that the direct incorporation of anthocyanins into biopolymer matrices can produce pH-sensitive films when these are developed through the casting methodology (Choi, Lee, Lacroix, & Han, 2017; Gutiérrez, 2018a; Liu et al., 2017; Luchese, Frick, Patzer, Spada, & Tessaro, 2015; Luchese, Garrido, Spada, Tessaro, & de la Caba, 2018; Ma & Wang, 2016; Pereira, de Arruda, & Stefani, 2015; Prietto et al., 2017; Yoshida, Maciel, Mendonça, & Franco, 2014). It is the bathochromic effect of the anthocyanins that makes these materials pH-sensitive, i.e. they change color depending on the pH of the medium.

One of the main advantages to using pH-sensitive films in food packaging is that they can alert the user to adulterations and contaminants in food, as well as informing him/her as to how fresh an item of food is or the duration of its shelf life, leading them to be dubbed “smart or intelligent” systems. This means that food packaging has become more than just a simple barrier to protect food, and is currently being developed as a warning system that could help to reduce the large amount of food that is wasted after harvesting (Gutiérrez & Alvarez, 2018).

In addition to characterizing the novel matrices used, this study focuses on investigating the biodegradability and compostability of the films developed. Frequently, studies assume that natural polymers are biodegradable and environmentally friendly. However, biodegradable materials are not necessarily compostable, and the international regulations that regulate these aspects in plastic materials are very clear (EN 13432, 2000; ASTM D5338 - 98, 2003; ISO 14855-1:2005, 2005; EN 14995, 2006; ISO 14855-2:2007, 2007). The current trend is towards the development of compostable materials, since they guarantee not only that the materials are biodegradable, i.e. they break down into small fragments, but also that the products of degradation do not represent a danger to the environment in terms of their ecotoxicity, i.e. they are compostable (Gutiérrez, 2018b). According to the ASTM D6400 (2004) standard, the methods for the evaluation of the ecotoxicity (compostability) of polymers are mainly based on the use of plants, soil fauna (earthworms), aquatic fauna (*Daphnia*), algae (green algae) and microbes (luminescent bacteria). However, we propose a new simple approach to evaluate the ecotoxicity of a polymer through an *in vivo* digestibility test using two biomarkers: weight change and survival in an insect. In this study we used the furniture weevil (*Tricorynus*

sp., Coleoptera: Anobiidae), one of the most serious pests of starches, flours and cereals in storage silos worldwide (FAO, 1985; Lovera, Pérez, & Laurentin, 2017).

The hypotheses of this research work were: 1) bionanocomposites developed from plum peel will enable the development of pH-sensitive films with better physicochemical and mechanical properties, and 2) weight changes and survival of the furniture weevil can be used as biomarkers for the evaluation of the compostability of the developed materials. Taking into account these hypotheses, the following objectives were defined: 1) exhaustively analyze the properties of the plastic materials developed, and 2) assess their biodegradability and compostability.

2. Experimental

2.1. Materials

Native pumpkin flour (*Cucurbita maxima*) from the edible part of the pumpkin and “huesito” plum (*Spondias purpurea*) flour from the fruit peel were obtained by the method described by Pacheco (2001). The pumpkins and plums were acquired at a local market in Caracas, Venezuela. The flours were stored in dark containers for one week at room temperature (25 °C) before preparing the films, in order to avoid oxidative damage to the materials used. Food grade glycerol (Aldrich, product code - G7893) was used as a plasticizer, and the plum flour as a nanocomposite.

2.2. Modifications to the pumpkin flour

The modification reactions carried out in this study were methylation and phosphorylation to the native (unmodified) pumpkin flour. It is well known that these reactions are more successful when carried out in an alkaline medium preferably pH = 10. All the modifications were thus performed at this pH value. It is important to note that modification by phosphorylation is approved by the U.S. Food and Drug Administration (FDA, 2017) for food applications, whereas modification by methylation is not. However, according to Sívoli et al. (2013), the latter has low cytotoxicity. The maximum concentration of the modifying agent allowed by the FDA (2017) for starchy matrices intended for the food industry (3% w/w of sodium trimetaphosphate (STMP - $\text{Na}_3\text{P}_3\text{O}_9$) with respect to the weight of the starchy matrix) was used. It is worth remembering that chemical reactions are given using molar ratios rather than weight or volume ratios. Thus, the same number of moles (0.0294 mol) of the modifying agent was used for both phosphorylation and methylation. The modifications were also performed using the same weight (300 g) of native pumpkin flour, and the same amount of solvent (300 mL of distilled water) so that the concentration of the modifying agent was the same for both reactions (0.098 M).

2.2.1. Modification by methylation (esterification)

Methylated pumpkin flour was obtained using dimethyl sulfate ($(\text{CH}_3)_2\text{SO}_4$) as a modifying agent using the procedure described by Sívoli et al. (2013). Briefly, native pumpkin flour (300 g) and 2.8 mL (0.0294 mol) of $(\text{CH}_3)_2\text{SO}_4$ were suspended in 300 mL of distilled water, and the pH adjusted to 10 with a 2.5% NaOH solution. The slurry was then heated to 45 °C and shaken for 3 h, with the pH adjusted every hour so that it remained at 10. After 3 h the pH was lowered to 7 with 2.5% HCl solution. The slurry was then washed three times by suspension in distilled water, centrifuged at 1500 r/min for 15 min, and dried in a tray dehydrator (Mitchell, USA, Model 645159) for 24 h at 45 °C. The dried modified flour was then milled and passed through a 60-mesh sieve. This same method was used for modification by phosphorylation, changing only the modifying agent employed.

2.2.2. Modification by phosphorylation (cross-linking)

Phosphated pumpkin flour was prepared with STMP as the

modifying agent using the method described by Kerr and Cleveland (1959) with some small adjustments following (Gutiérrez, Morales, et al., 2015).

2.3. Characterization of the modified matrices and the nanocomposite (plum flour)

Moisture content, fat, ash and crude protein (N x 6.25) (obtained by the micro-Kjeldahl procedure) were calculated using official methods (AACC, 2003). Crude fiber was determined by the method proposed by Van Soest and Wine (1967). Total amylose content was measured by differential scanning calorimetry (DSC) as described by Mestres, Matencio, Pons, Yajid, and Flidel (1996) and Amani, Buléon, Kamenan, and Colonna (2004), which is based on the energy used during the formation of the amylose/lyso-phospholipid complex. The total carbohydrate content of the flours was calculated by subtracting the percentages of water content, ash, crude protein and fatty materials from one hundred percent of sample. The phosphorus content and degree of substitution (DS) were determined by the colorimetric method (FAO, 2007) using the equations proposed by Deetae et al. (2008). Total anthocyanins in the plum flour were determined according to the method proposed by Hassimotto, Mota, Cordenunsi, and Lajolo (2008). Anthocyanin concentration was expressed as mg of pigment/100 g of sample. Absorbance of the patterns and samples was measured at 532 nm. All procedures were performed in triplicate. The results were reported as the mean values \pm standard deviation (SD).

2.4. Film formation

Films were prepared by the casting methodology from each of the two modified pumpkin flours using 5% w/v of flour, 1.9% w/v of glycerol and 500 mL of distilled water. The film-forming solutions (FFS) were heated for 30 min at 90 °C in a water bath with constant stirring to ensure gelatinization (Gutiérrez & Álvarez, 2016). Plum flour was added to some of the films at 4% w/w with respect to the weight of matrix 2 min before the end of the FFS process in order to preserve the anthocyanins (pigments) and to ensure a homogeneous distribution of the nanocomposite. After gelatinization the FFS were degassed for 30 min by applying a vacuum. They were then poured into 40 x 30 cm stainless steel trays maintaining a constant level and uniform thickness, and left in a tray dehydrator (Mitchell, USA, Model 645159) for 24 h at 45 °C. Once dried the four thermoplastic flour (TPF) film systems: phosphorylated pumpkin flour (TPF-PPF), phosphorylated pumpkin flour/plum flour (TPF-PPF/P), methylated pumpkin flour (TPF-MPF) and methylated pumpkin flour/plum flour (TPF-MPF/P) were peeled off the trays. The resultant materials were conditioned with a saturated solution of NaBr ($a_w \sim 0.575$ at 25 °C) for seven days prior to each test. During this period the containers were protected from light in a dark room in order to avoid photodegradation of the pigments.

2.5. Film characterization

2.5.1. Optical microscopy

Small pieces (2 cm x 1 cm) of each film system were mounted onto glass slides and observed with an optical microscope (Olympus BX60M, Japan) at 50x. A video camera imaging system (Olympus IMAGE RS) was used to examine and photograph the film surfaces exposed to the drying air. At least three microphotographs of each system were taken.

2.5.2. Atomic force microscopy (AFM)

The film surfaces exposed to the drying air were examined, and topographic images of the films obtained using an Agilent 5500 in the Acoustic AC Mode (AAC Mode) with silicon nitride (Si_3N_4) tips and a cantilever oscillation frequency of 155 kHz. The tips were 2 mm long and V-shaped with a spring constant of 0.2 N/m, and were positioned over the sample under ambient conditions. AFM images were taken at

both the center and periphery of the surface of the films and processed with PicoView image software. The average roughness (Ra) of the exposed dried surfaces was also assessed.

2.5.3. Water contact angle (WCA)

To determine the water contact angles (WCA) a drop of distilled water (2 μL) was placed on the surface exposed to the drying air during film preparation. The WCA were then measured at 25 °C using an USB Digital Microscope (model DIGMIC200X, China) equipped with an Image Analysis Software 220X 2.0MP video, with 0.01° precision. The WCA were acquired taking note of the recommendations made by Gutiérrez and González (2016) in order to avoid false results caused by phenomena such as dehydration, swelling and dissolution. A total of 12 WCAs were measured per film.

2.5.4. Moisture content (MC)

The moisture content of the different film systems was calculated using the methodology described by AOAC (1990) and the following equation:

$$MC (\%) = \frac{m_w - m_d}{m_w} \times 100 \quad (1)$$

where m_w is the wet mass and m_d the dry mass of each film system.

The dry mass of the films was determined by cutting samples of each system into 2 x 2 cm pieces, heating them in an oven at 105 °C for 24 h, and then weighing each one with an analytical balance (Denver Instrument APX-200). Analyses were performed in triplicate and the % moisture content \pm SD was reported.

2.5.5. Water solubility (WS)

Water solubility (WS) was determined according to the method described by Gutiérrez and Alvarez (2017c). Samples of each film were cut into 2 x 2 cm pieces and the initial weights registered (w_i). The initial dry matter content of each film system was then determined by drying them to a constant weight in an oven (Memmert, Germany) at 105 °C for 24 h. To determine the weight of the dry matter not solubilized in water the film pieces were immersed in 50 mL of distilled water and stored for 24 h at 25 °C. After this, they were filtered through previously desiccated and weighed filter paper, and the undissolved films obtained dried again to a constant weight (w_f) in the same oven at 105 °C for 24 h. The solubility of each film system was then calculated as follows:

$$WS (\%) = (w_i - w_f) \times w_i^{-1} \times 100 \quad (2)$$

where w_i and w_f are the initial and final weights of each sample, respectively. Results were reported as % water solubility \pm SD from three measurements per film system.

2.5.6. X-ray diffraction (XRD)

X-ray diffractograms of the different film systems were acquired using an X-ray diffractometer (Siemens D 5000) (monochromatic $\text{Cu K}\alpha$ radiation source - $\lambda = 1.5406 \text{ \AA}$) operating at a voltage of 40 kV and current 30 mA. Scattered radiation was detected in a 2θ angular range from 3 to 33° at a scanning rate of 1°/min. The distances between the planes of the crystals d (\AA) were calculated from the diffraction angles ($^\circ$) measured from the X-ray diffractograms according to Bragg's law:

$$n\lambda = 2d \sin(\theta) \quad (3)$$

where λ is the $\text{Cu K}\alpha$ radiation wavelength, and n the order of reflection. For the calculations n was taken as 1. The thicknesses of the samples on the slides were $\sim 0.84 \text{ mm}$. In each case the crystalline fraction was estimated as the area above the smooth curve drawn between the main peaks (main d -spacings) (Hermans & Weidinger, 1961).

2.5.7. Thermogravimetric analysis (TGA)

The thermogravimetric tests were done with a thermal analyzer

(Shimadzu DTG-60, Japan). Samples were heated at a constant rate of 10 °C/min from room temperature to 500 °C under a nitrogen flow of 30 mL/min. Film weights were in the range of 7–13 mg. Three replicates per sample were analyzed to ensure repeatability. The residual mass of the materials was recalculated on dry basis and the different degradation phases noted. The SD was lower than 1% for all the systems tested, and the representative curves of each one were reported.

2.5.8. Differential scanning calorimetry (DSC)

The DSC thermograms were acquired by a Mettler Toledo DSC 823, (Schwerzenbach, Switzerland) and used to determine the glass transition temperatures (T_g) and enthalpies (ΔH) of all the films under study. The T_g was measured as the temperature in the middle of the relaxation range and the ΔH as the difference in heat flow. Samples of 6–7 mg were weighed, placed individually in aluminum pans and hermetically sealed; an empty pan was used as a reference. Initially, samples were heated at a rate of 20 °C/min from 30 °C to 120 °C under nitrogen atmosphere to remove previous thermal history and moisture (Gutiérrez, Herniou-Julien, Álvarez, & Álvarez, 2018). They were then cooled down to –70 °C using an intracooler and re-heated to 120 °C at a heating rate of 10 °C/min. Two samples of each film system were tested to ensure repeatability. All the thermograms shown refer to the second heating.

2.5.9. Field emission scanning electron microscopy (FESEM)

A FESEM Supra55, Zeiss (Oberkochen, Germany) operating at an acceleration voltage of 3 kV was used to analyze the fracture surface of each film system. The films were previously cryofractured by immersion in liquid nitrogen, mounted on bronze stubs and sputter coated (Sputter coater SPI Module, Santa Clara, CA, USA) with a thin layer of gold for 35 s. All samples were observed at a magnification of 1 k \times .

2.5.10. Uniaxial tensile tests

An Instron dynamometer (Instron Ltd., High Wycombe, UK) (5 Lbs) working at a speed of 0.02 in/sec was used to obtain the stress-distance curves of the film systems evaluated. At least ten specimens of each system with an effective length of 10 mm and width 0.5 mm were tested at room temperature (25 °C) following the ISO 527-2 (2012) norm. The stress-distance curves were then transformed into stress-strain curves to determine the different mechanical properties: Young's modulus (E), maximum stress (σ_m), strain at break (ϵ_b) and toughness (T). The elastic modulus or Young's modulus was measured from the slope of the linear regression of the stress-strain curves where the maximum stress value is the maximum point of each curve, and the strain at break corresponds to the maximum elongation of the samples before rupture. Toughness was determined as the area under the stress-strain curves.

2.5.11. Response to pH changes

In order to evaluate the responses of the films to pH changes, square samples (25 \times 25 mm) of each system were placed in solutions at pHs of either 1, 7 or 13, prepared from HCl (0.1 M) and NaOH (0.1 M). Film response was then evaluated from images taken with an 8.1 mega pixel Cyber-shot Sony camera; model DSC-H3 (Tokyo, Japan).

2.5.12. Stability in acidic or alkaline solutions

The stability of the films in acidic and alkaline solutions was evaluated by immersing film pieces (25 \times 25 mm) in containers with 20 mL of either standard HCl (pH 1) or NaOH (pH 13) solution. The containers were then sealed and maintained at 25 °C for 24 days. Changes in the appearance of samples were recorded with an 8.1 mega pixel Cyber-shot Sony camera, model DSC-H3 (Japan). At least six samples of each film system were tested in order to ensure good reproducibility.

2.5.13. Biodegradability in vegetable compost

The biodegradability of the films developed was studied using a procedure developed by our research group (Medina Jaramillo,

Gutiérrez, Goyanes, Bernal, & Famá, 2016). Briefly, the vegetable compost (soil) was crushed and sieved to remove conglomerates. It was then tipped into aluminum containers up to a height of approx. 5 cm. Discs (12 mm diameter) of each film system were then cut and weighed on dry basis to give the initial mass of the film before the test (m_i). The m_i was determined by heating the discs in an oven at 105 °C for 24 h, and then weighing each one with an analytical balance (Denver Instrument APX-200). The discs were then buried in the compost (one disc per film system in each container) at a depth of approx. 10 mm. On days 2, 4, 6 and 8 after the start day (day 0) one of the containers was unearthed and, where possible, the dry mass of each of the discs was recorded (m_f). The percentage of biodegradability was then estimated as follows:

$$\text{Biodegradability}(\%) = \frac{m_i - m_f}{m_i} \times 100 \quad (4)$$

The tests were carried out at room temperature (30 °C) and controlled humidity conditions (70–80%). Analyses were performed in triplicate and % biodegradability \pm SD was reported.

2.5.14. In vivo digestibility tests as an ecotoxicity bioassay

The ecotoxicity of films was estimated using the furniture weevil (*Tricorynus* sp, Coleoptera: Anobiidae). Two ecotoxicity biomarkers were evaluated: survival and changes in weight.

2.5.14.1. Furniture weevil culture & diet preparation. The weevils were maintained using the methodology described by Lovera et al. (2017). The films were dried in an oven at 105 °C for 72 h before milling and passing them through a 60-mesh sieve. This was done to avoid distortions in the results due to variations in the moisture content of the films, as well as to guarantee a particle size that did not affect the values of the evaluated biomarkers.

2.5.14.2. Survival & weight changes of the weevils. To carry out the bioassays weevils were deposited in four recipients (30 weevils per recipient) and fed with 3 g of the previously prepared diets. The recipients were covered with a mesh to prevent the insects from escaping. Bioassays were performed at room temperature (30 °C) over a period of 8 days. Every two days the weevils were weighed and any dead ones discarded. The tests were carried out in triplicate. The biomarkers were then calculated using equations (5) and (6):

$$\text{Survival}(\%) = \frac{Nlw}{Inw} \times 100 \quad (5)$$

where Nlw = number of live weevils on day “n” and Inw = initial number of weevils.

$$\text{Weight change}(\%) = \frac{W_f - W_i}{W_i} \times 100 \quad (6)$$

where W_i = initial average weight and W_f = average weight on day “n”.

2.6. Statistical analysis

The data was examined by analyses of variance (ANOVA) using OriginPro 8 (Version 8.5, Northampton, USA) software, and the results shown as average values \pm SD. Significant differences between the mean values of the measured properties were compared using a multiple-range Tukey's test. A significance level of 0.05 was used.

3. Results and discussion

3.1. Characterization of the modified matrices and the plum flour nanocomposite

Table 1 shows the results of the proximal analysis of the biomatrices and the nanocomposite. The phosphated pumpkin flour (PPF) had a

Table 1
Chemical composition on dry basis of the different flours studied.

Parameter	PPF	MPF	PF
Moisture (%)	15 ± 3 ^{a,b}	9 ± 1 ^a	13 ± 4 ^a
Crude protein (%)	4.29 ± 0.04 ^c	3.05 ± 0.02 ^a	3.4 ± 0.2 ^b
Crude fat (%)	0.39 ± 0.05 ^a	0.2 ± 0.2 ^a	0.8 ± 0.1 ^b
Ash (%)	13.33 ± 0.03 ^b	32.99 ± 0.06 ^c	2.55 ± 0.01 ^a
Crude fiber (%)	4.4 ± 0.3 ^b	3.5 ± 0.5 ^a	3.4 ± 0.1 ^a
Total carbohydrates (%)	70.0 ± 0.1 ^b	54.8 ± 0.1 ^a	80.2 ± 0.1 ^c
Total amylose (%)	20 ± 9 ^a	18 ± 9 ^a	N.
P (%)	0.27 ± 0.02 ^b	0.019 ± 0.009 ^a	0.022 ± 0.004 ^a
Degree of substitution	0.028 ± 0.002 ^a	N.d.	N.d.
Anthocyanins (mg/100 g)	0 ± 0 ^a	0 ± 0 ^a	50.7 ± 0.8 ^b

Similar superscript letters in the same row indicate no statistically significant difference ($n = 3$, $p \leq 0.05$). Abbreviation: phosphated pumpkin flour (PPF), methylated pumpkin flour (MPF) and plum flour (PF).

N.d. = Not determined.

N. = Negligible.

significantly higher moisture content ($p \leq 0.05$) than the methylated pumpkin flour (MPF). This is because modification by methylation reduces the water sensitivity of the biomatrix due to the introduction of apolar functional groups (methyl groups - CH_3). The moisture contents of the PPF and the plum flour (PF) were similar (between 13 and 15%). Comparable results have been reported by Jay (1995) for other starchy matrices with a stable lifespan. The PPF showed the highest crude protein content (4.29%), and the PF the highest crude fat content (0.8%). No statistically significant differences ($p \geq 0.05$) in the crude fat content were, however, observed between the PPF and MPF. The highest ash content was recorded for the MPF (32.99%). According to Gutiérrez (2018c) the high ash content in methylated plantain flour may be associated with the production of barium sulfate (BaSO_4) as a by-product of the methylation reaction. The crude fiber content was never higher than 4.4%: PPF ($4.4 \pm 0.3\%$) > MPF ($3.5 \pm 0.5\%$) \approx PF ($3.4 \pm 0.1\%$), and no significant differences ($p \geq 0.05$) were observed between the total amylose contents of the PPF and MPF. It is worth noting that although a methodology commonly used to quantify total amylose content was employed (based on the energy used during the formation of the amylose/lyso-phospholipid complex) the values obtained must be taken as apparent amylose content since the fat content of the matrices can hinder exact quantification (Gutiérrez, 2018c). No amylose content was recorded for the PF. This means that the PF does not contain starch and that the total carbohydrate content in this biopolymer consists of non-starch carbohydrates. As expected, the phosphated matrix showed the highest phosphorus content (0.27%). The degree of substitution (DS) by phosphating was 0.028 for the PPF, thus confirming that the cross-linking reaction by phosphating using sodium trimetaphosphate (STMP - $\text{Na}_3\text{P}_3\text{O}_9$) as a modifying agent did take place. A content of 50.7 mg/100 g of anthocyanins was registered for the PF.

3.2. Film characterization

3.2.1. Optical microscopy & atomic force microscopy (AFM)

The optical micrographs of the films evaluated confirm that the materials were totally plasticized (Fig. 1). The films manufactured from methylated pumpkin flour (TPF-MPF and TPF-MPF/P, Fig. 1 c and d) were qualitatively more yellowish and opaque than their phosphated analogs (TPF-PPF and TPF-PPF/P, Fig. 1 a and b). Similarly, the films with added plum flour (TPF-PPF/P and TPF-MPF/P, Fig. 1 b and d) as a nanocomposite were qualitatively more opaque than those without the plum flour nanocomposite (TPF-PPF and TPF-MPF, Fig. 1 b and d). Similar results have been reported by other authors after adding amaranth starch nanocomposites to reinforce amaranth protein films (Condés, Añón, Dufresne, & Mauri, 2018).

The AFM observations of the film surfaces (Fig. 2) gave the following average roughness (Ra) values: 140 nm, 25 nm, 160 nm, and 130 nm for the TPF-PPF, TPF-PPF/P, TPF-MPF and TPF-MPF/P films, respectively. These results show that the films prepared from the methylated pumpkin flour (TPF-MPF and TPF-MPF/P, Fig. 2) were rougher than those made from the phosphated pumpkin flour (TPF-PPF and TPF-PPF/P, Fig. 2) and that the addition of the plum flour as a nanocomposite decreased the Ra values independently of the modifying agent used. A decrease in Ra values by adding beet flour as a nanofiller to films derived from native and phosphated plantain flour was reported by Gutiérrez, Suniaga, Monsalve, and García (2016). It is worth noting that the plum flour nanocomposite had a particle size of approx. 200 nm. This was especially evident from the AFM image of the TPF-PPF/P film (Fig. 2).

3.2.2. Water contact angle (WCA), moisture content (MC) & water solubility (WS)

Higher water contact angle (WCA) values (Fig. 3) accompanied by low water solubility (WS) values (Table 2) confirm that the methylation modification of the pumpkin flour resulted in less hydrophilic materials (TPF-MPF and TPF-MPF/P), i.e. materials that are less sensitive to water, than those obtained from the modification by phosphation (TPF-PPF and TPF-PPF/P). However, there were no significant differences ($p \geq 0.05$) between the moisture content (MC) values (Table 2) of the modified films. The WCA and WS results were expected since the introduction of methyl groups within the pumpkin flour biomatrix reduces the number of hydroxyl groups capable of scavenging moisture (Lewis sites, polar sites). In contrast, the introduction of phosphate groups to the biopolymer matrix, despite being polar, has been shown to reduce sensitivity to water in biopolymer-based films due to the compensation of the Lewis sites. This is mainly due to the hydrogen bonding interactions between the phosphate groups and the glycerol (plasticizer) or the phosphate groups and the biopolymer matrix (Gutiérrez, Tapia, Pérez, & Famá, 2015). Thus, apparently, a greater reduction in hydrophilicity is caused by apolar chemical modification by methylation than by the compensation of the polar sites by phosphation.

The addition of a nanocomposite to biopolymeric films frequently leads to a decrease in their hydrophilicity (Álvarez, Famá, & Gutiérrez, 2017). In this study, however, no statistically significant differences ($p \geq 0.05$) in the MC and WS values between the nanocomposite-containing films (TPF-PPF/P and TPF-MPF/P) and their analogous films without the nanocomposite (TPF-PPF and TPF-MPF) were observed. This suggests that in this case the nanocomposite did not significantly reduce the hydrophilicity of the materials obtained. The WCA of the methylated pumpkin film plus nanocomposite (TPF-MPF/P) was significantly higher ($75 \pm 4^\circ$) ($p \leq 0.05$) than that of the methylated pumpkin film without the nanocomposite ($56 \pm 6^\circ$; TPF-MPF), whereas the incorporation of the plum flour nanocomposite in the phosphated pumpkin flour-based film did not significantly alter its WCA. Thus, the addition of the nanocomposite increased the hydrophobicity only superficially in the methylated pumpkin flour film.

Several authors have associated the surface morphology of biopolymer-derived films with their WCA values. Specifically, Sengupta and Han (2014) and Gutiérrez, Ollier, and Alvarez (2018) showed that higher WCA values correlate with rougher surfaces due to the fact that surface irregularities act as physical obstacles that prevent surface wetting. This fits well with the surface morphologies observed and the WCA values obtained for both the phosphated and the methylated films. However, the behavior described by Sengupta and Han (2014) and Gutiérrez, Ollier, et al. (2018) fails to explain what happened when the nanocomposite was added to the biomatrices, especially with regard to the methylated flour films (TPF-MPF and TPF-MPF/P). Similar results were reported by Gutiérrez and González (2017) for films prepared from plantain flour cross-linked with *aloe vera* gel. In fact, taking the results of Gutiérrez and González (2017) into account we can say

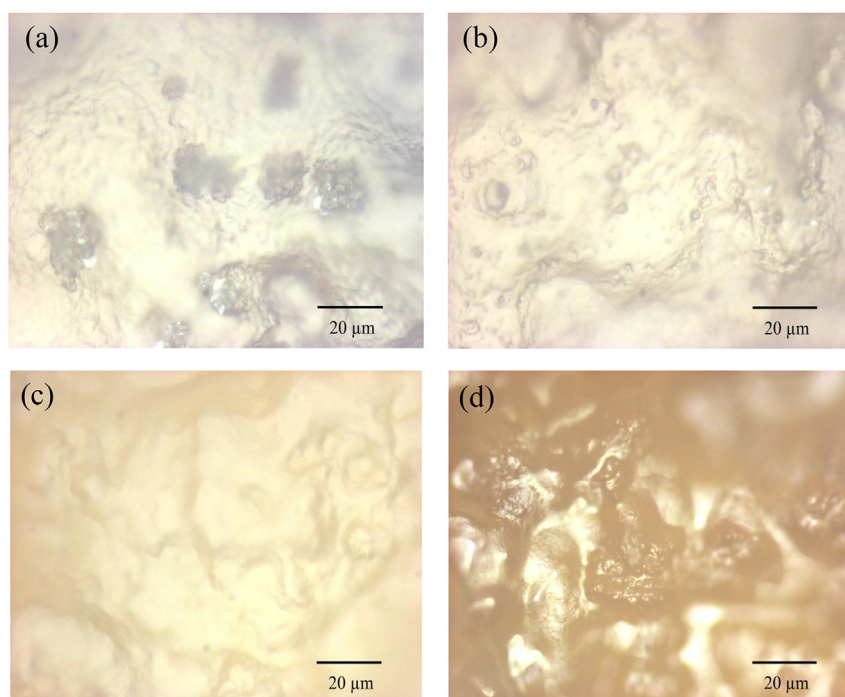


Fig. 1. Optical micrographs of the films based on: (a) phosphated pumpkin flour (TPF-PPF), (b) phosphated pumpkin flour/plum flour (TPF-PPF/P), (c) methylated pumpkin flour (TPF-MPF) and (d) methylated pumpkin flour/plum flour (TPF-MPF/P). At 50 × of magnification.

that the higher WCA values in the TPF-MPF/P system as compared to the TPF-MPF system could be associated with strong chemical interactions located below the surface of the film. These interactions would prevent Lewis sites from being available (and thus producing the collapse of the water drop on the surface) and explains why, despite the fact that the surface of the TPF-MPF/P film is smoother than that of the TPF-MPF film, the former had a significantly higher WCA than the latter.

3.2.3. X-ray diffraction (XRD)

The X-ray diffractograms (Fig. 4) of the developed films showed the characteristic peaks of the crystalline phase of the biopolymeric material. Specifically, the TPF-PPF film displayed peaks at $2\theta = 22.0^\circ$ and 24.5° , corresponding to the d -spacings $\cong 4.1 \text{ \AA}$ and 3.7 \AA , respectively, indicating the presence of A and B type structures. In contrast, the TPF-PPF/P film (i.e. the one with the added nanocomposite) showed a slight shift of the peaks mentioned above to lower 2θ values. This suggests that the addition of the plum flour nanocomposite produced an increase in the molar volume of the phosphated film (TPF-PPF/P > TPF-PPF). Similar results were reported by Gutiérrez and Alvarez (2017c) for eco-friendly films prepared from plantain flour/poly (ϵ -caprolactone) (PCL) blends under reactive extrusion conditions. Taking into account the results given by Gutiérrez and Alvarez (2017c), this slight increase in the molar volume can be directly related to a V-type structure, i.e. to the hydrogen bond interactions between the starch and glycerol.

Other additional peaks were observed in the phosphated pumpkin flour-based films (TPF-PPF and TPF-PPF/P), for example, the peaks located at $2\theta = 17.0^\circ$ (5.2 \AA) and 18.2° (4.9 \AA), which confirm the existence of A and B type structures. According to García-Tejeda et al. (2013) $2\theta = 17.0^\circ$ is associated with interactions between the short external amylopectin chains and the glycerol. It is worth noting that unlike the TPF-PPF film, the TPF-PPF/P film also showed the V-type structure (peaks at $2\theta = 20.0^\circ$ (4.4 \AA) and 20.4° (4.3 \AA)). It has been established in the literature that the V-type structure corresponds to glycerol-starch hydrogen bonding interactions (Gutiérrez & González, 2016). Our results thus confirm that the plum flour nanocomposite generates hydrogen bonding interactions with the phosphated matrix.

Interestingly, the methylated pumpkin flour-based films showed very high crystallinity values (TPF-MPF – 89.1% and TPF-MPF/P – 94.0%); the highest for all the films in this study and typical of extremely crystalline materials. These films (TPF-MPF and TPF-MPF/P) also showed similar spectra to that of BaSO_4 (Ramaswamy, Vimalathithan, & Ponnusamy, 2010). This confirms that the methylation modification generates large quantities of BaSO_4 as a reaction by-product. In contrast, the phosphated pumpkin flour-based films (TPF-PPF – 29.5% and TPF-PPF/P – 36.2%) exhibited crystallinity values typical of semicrystalline materials, i.e. they were mainly amorphous with a weak crystalline phase. Finally, the addition of the plum flour to the matrices increased the crystallinity values with respect to their analogous films that did not contain the nanocomposite.

3.2.4. Thermogravimetric analysis (TGA)

The TGA curves of the systems evaluated (Fig. 5) exhibited three stages of thermal degradation: 1) the evaporation of adsorbed moisture and free water within the material (occurs between 50 and 100°C). It is worth noting that this stage was not evident from Fig. 5, since the curves were plotted as a function of the residual mass on dry basis in order to avoid distortions in the results as a consequence of the different moisture content values of the systems under study; 2) evaporation of the glycerol-rich phase, which also contains starch (occurs from 160°C , with a maximum evaporation temperature at 290°C). It should be noted that during this step, part of the starch contained in the glycerol-rich phase also decomposes; 3) decomposition of the starch rich phase (occurs from 300 or 320°C) (Gutiérrez, Morales, et al., 2015). According to Zeppa, Gouanvé, and Espuche (2009) during the last stage of thermal degradation the polyhydroxyl groups of the starch are eliminated and the thermoplastic starch (TPS) matrix undergoes depolymerization and decomposition, followed by the production of carbon.

It can also be observed from Fig. 5 that the methylated pumpkin flour-based films (TPF-MPF and TPF-MPF/P) showed higher thermal resistances than the phosphated pumpkin flour-based films (TPF-PPF and TPF-PPF/P). A higher thermal resistance was also observed for the TPF-PPF/P film compared to the TPF-PPF film, i.e. the addition of the nanocomposite led to an increase in the thermal resistance of the

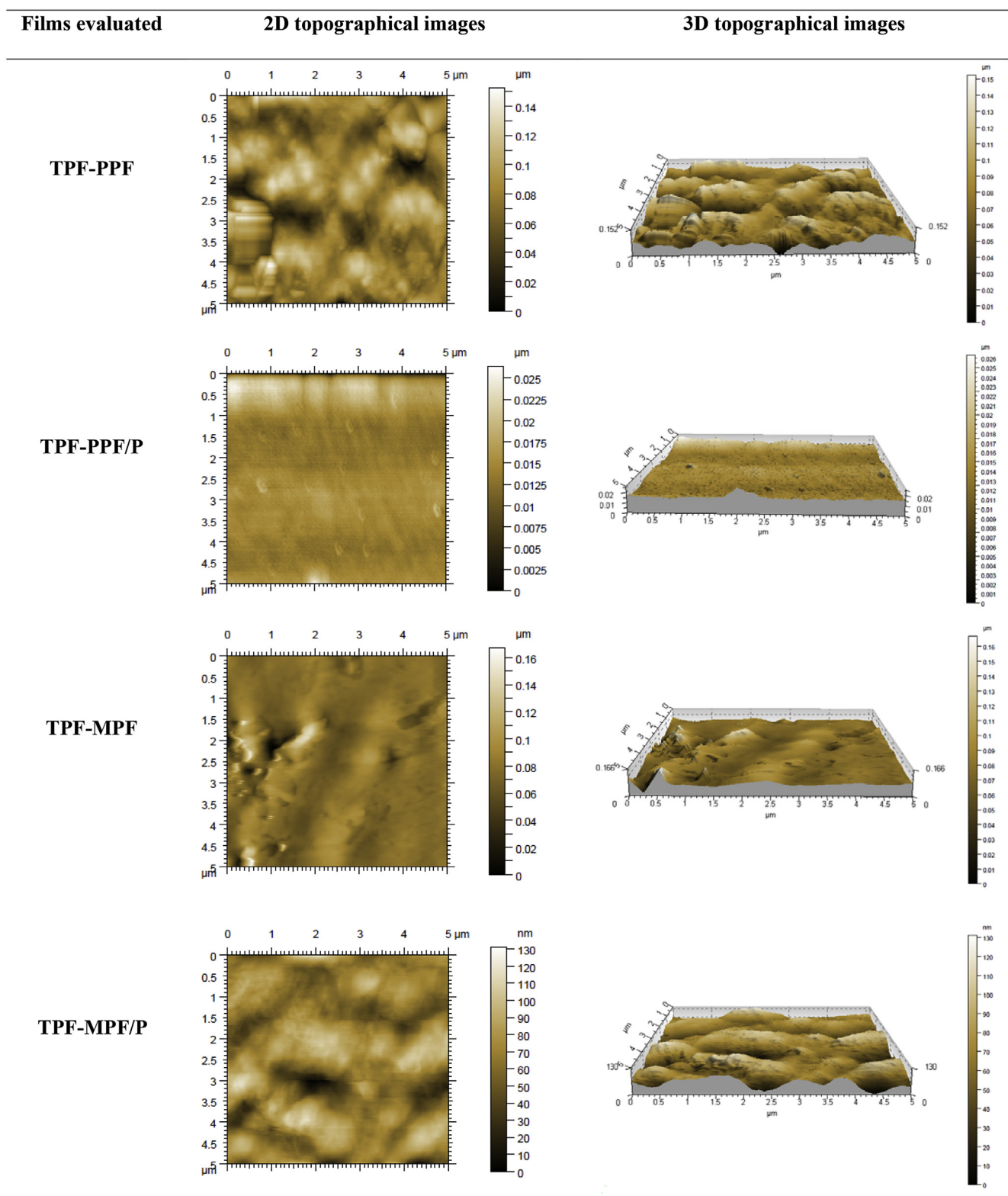


Fig. 2. AFM images of the surface of the films based on: phosphated pumpkin flour (TPF-PPF), phosphated pumpkin flour/plum flour (TPF-PPF/P), methylated pumpkin flour (TPF-MPF) and methylated pumpkin flour/plum flour (TPF-MPF/P).

phosphated material. This is probably due to the hydrogen bond interactions between the nanocomposite and the phosphated matrix, and is in line with the results obtained from the XDR diffractograms (see section 3.2.3). The opposite effect was observed in the methylated films where the addition of the nanocomposite decreased the thermal resistance of the methylated material.

The residual mass of the methylated pumpkin flour-based films (TPF-MPF and TPF-MPF/P, approx. 40.52%) was higher than that of the phosphated pumpkin flour-based films (TPF-PPF and TPF-PPF/P, approx. 28.28%) in the last stage of thermal degradation. This is possibly due to the high ash content of the methylated matrix (see section 3.1) associated with the presence of BaSO₄ as a by-product of the

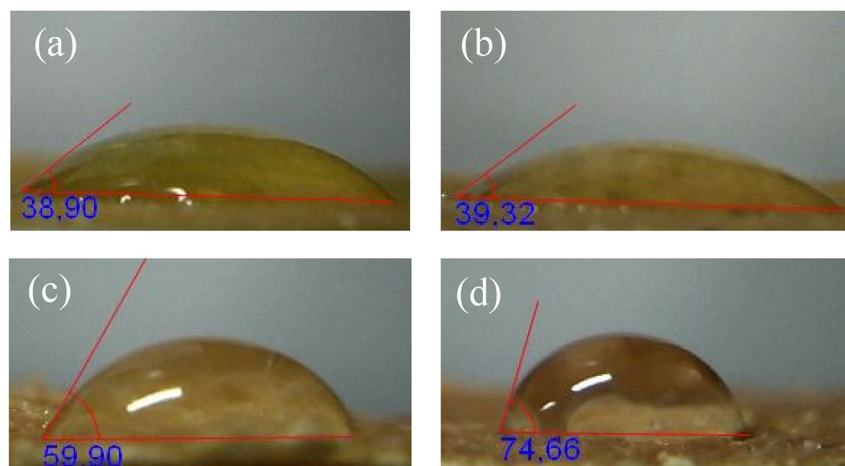


Fig. 3. Water contact angles of the different films studied based on: (a) phosphated pumpkin flour (TPF-PPF), (b) phosphated pumpkin flour/plum flour (TPF-PPF/P), (c) methylated pumpkin flour (TPF-MPF) and (d) methylated pumpkin flour/plum flour (TPF-MPF/P).

Table 2

Water contact angle (WCA), moisture content (MC) and water solubility (WS) of the different films evaluated.

Parameters	TPF-PPF	TPF-PPF/P	TPF-MPF	TPF-MPF/P
WCA (°)	39 ± 3 ^a	38 ± 3 ^a	56 ± 6 ^b	75 ± 4 ^c
MC (%)	29 ± 3 ^{a,b}	27 ± 2 ^a	24 ± 4 ^a	23 ± 2 ^a
WS (%)	75 ± 3 ^b	72 ± 1 ^b	50.1 ± 0.7 ^a	51 ± 1 ^a

Equal letters in the same row indicate no statistically significant differences ($p \leq 0.05$).

Film systems based on: phosphated pumpkin flour (TPF-PPF), phosphated pumpkin flour/plum flour (TPF-PPF/P), methylated pumpkin flour (TPF-MPF) and methylated pumpkin flour/plum flour (TPF-MPF/P).

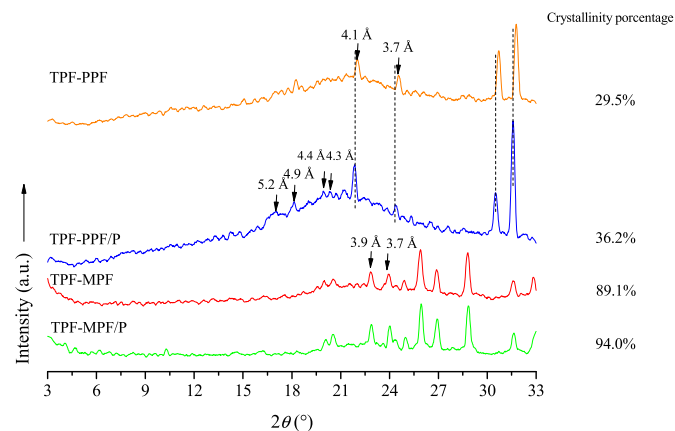


Fig. 4. X-ray diffraction patterns of the different films based on: phosphated pumpkin flour (TPF-PPF), phosphated pumpkin flour/plum flour (TPF-PPF/P), methylated pumpkin flour (TPF-MPF) and methylated pumpkin flour/plum flour (TPF-MPF/P).

methylation reaction (see section 3.2.3).

3.2.5. Differential scanning calorimetry (DSC)

The thermograms illustrated in Fig. 6 show that the methylated pumpkin flour-based films (TPF-MPF and TPF-MPF/P) had higher glass transition temperature values (T_g) than their phosphated analogs (TPF-PPF and TPF-PPF/P). This suggests that phosphated films behave as plastics whereas methylated films do not. In addition, the higher T_g values for the TPF-MPF and TPF-MPF/P films compared to their phosphated analogs (TPF-PPF and TPF-PPF/P) can be associated with the higher thermal resistance of the methylated materials (see TGA

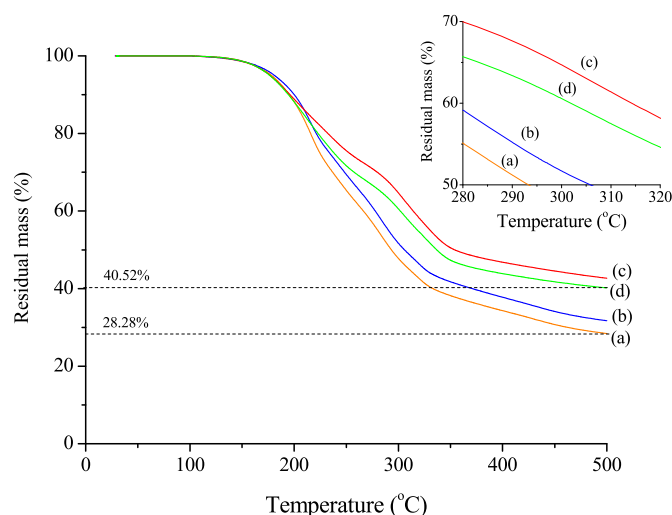


Fig. 5. TGA curves of the different films studied based on: (a) phosphated pumpkin flour (TPF-PPF), (b) phosphated pumpkin flour/plum flour (TPF-PPF/P), (c) methylated pumpkin flour (TPF-MPF) and (d) methylated pumpkin flour/plum flour (TPF-MPF/P).

curves, section 3.2.4).

It is well known that an increase in T_g values may also be related to physical impediments that reduce the mobility of the polymer chains (Gutiérrez & Alvarez, 2017c). The T_g values in the film systems with the added nanocomposite were higher than those of their analogs without it. These results were expected as one of the jobs of the nanocomposite filler is to reinforce the matrix in order to harden and stiffen the films.

3.2.6. Field emission scanning electron microscopy (FESEM) & uniaxial tensile tests

The FESEM micrographs (Fig. 7) of the cryogenic fracture surfaces of the methylated pumpkin flour-based films (TPF-MPF - Fig. 7 c and TPF-MPF/P - Fig. 7 d) showed a porous morphology demonstrating that they have poor adhesive strength compared to the phosphated pumpkin flour-based films (TPF-PPF - Fig. 7 a and TPF-PPF/P - Fig. 7 b), which had cryogenic fracture surfaces with a more compact morphology. In addition, TPF-PPF/P film (Fig. 7 b) evidences the incorporation of the plum flour nanocomposites within the polymeric matrix compared to the TPF-PPF film (i.e. without added nanocomposite, Fig. 7 a). The uniaxial tensile test results revealed that the films with a more compact morphology (TPF-PPF and TPF-PPF/P, Fig. 7 a and b, respectively) had improved mechanical properties (Table 3). In contrast, the methylated

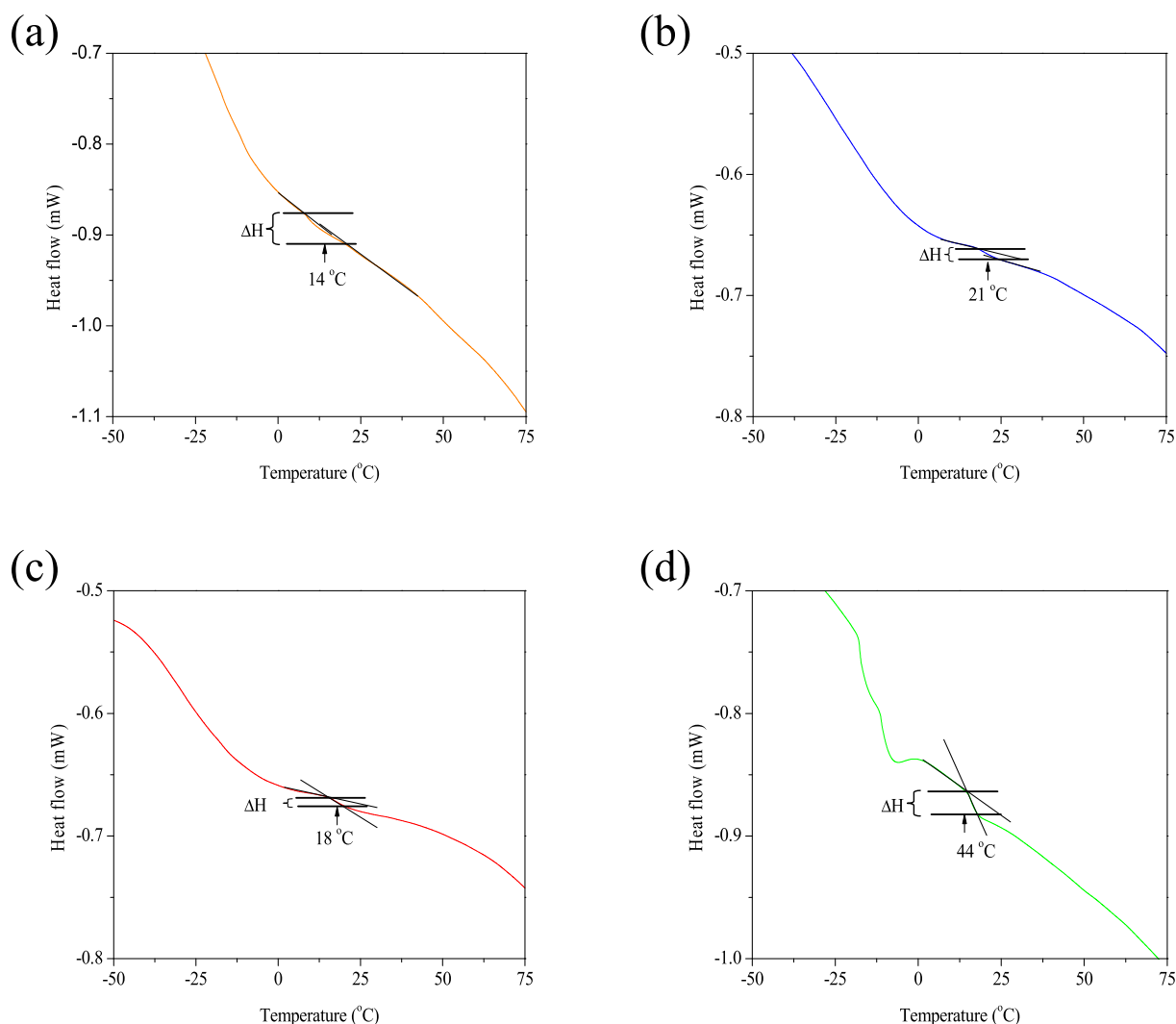


Fig. 6. Heating thermograms of the films based on: (a) phosphated pumpkin flour (TPF-PPF), (b) phosphated pumpkin flour/plum flour (TPF-PPF/P), (c) methylated pumpkin flour (TPF-MPF) and (d) methylated pumpkin flour/plum flour (TPF-MPF/P).

pumpkin flour-based films (TPF-MPF and TPF-MPF/P, Fig. 7 c and d, respectively) were so fragile and with a porous morphology that they could not be tested.

The results discussed so far thus indicate that modification by methylation of the biopolymer matrix can reduce sensitivity to water and increase the thermal resistance of bio-based materials. The large scale application of these materials would, however, be limited by their fragility. Fig. 8 shows that the addition of the plum flour nanocomposite in the TPF-PPF/P film fulfilled the aim of reinforcing the polymer matrix, since the mechanical parameters: Young's modulus (E), maximum stress (σ_m) and strain at break (ϵ_b) were significantly higher ($p \leq 0.05$) (at least twice as high) in this system than those registered for the TPF-PPF film (i.e. without the added nanocomposite) (Table 3). This is probably because the hydrogen bonding interactions between the nanocomposite and the phosphated matrix produce a material with a ductile mechanical behavior.

Finally, the phosphated films showed a more plastic behavior than the methylated films and the addition of the nanocomposite produced a more rigid and hardened material. This fits well with the DSC results (see section 3.2.5).

3.2.7. Response to pH changes & stability in acidic or alkaline solutions

The films containing the plum flour nanocomposite (TPF-PPF/P and TPF-MPF/P, Fig. 9) unfortunately did not show the expected

bathochromic (pH-sensitive) effect. This is probably because the anthocyanins (pH-sensitive active compounds) contained in the plum flour nanocomposite were compromised. As regards the stability of the films in acidic or alkaline solutions, the TPF-MPF and TPF-MPF/P systems were less stable in the acid medium than the TPF-PPF and TPF-PPF/P systems after 24 days of immersion (Fig. 10). This may be because the more porous morphology of the methylated film systems (Fig. 7 c and d) enabled the acidic solution (HCl) to reach the interior of the materials more easily, leading to their rapid disintegration. It is worth noting that the TPF-PPF/P film was more swollen than the TPF-PPF film after 24 days immersed in the acidic medium, i.e. the presence of the nanocomposite increased the tendency of the phosphated film system to swell. The greater degree of swelling of the TPF-PPF/P film compared to the TPF-PPF film could be due to the greater molar volume of the former compared to the latter (see section 3.2.3). This increase in molar volume would also enable the acidic solution (HCl) to penetrate the structure of the material more easily causing it to swell.

It can be observed from Fig. 11 that the TPF-PPF and TPF-PPF/P films were more stable in the alkaline medium after 17 days of immersion than the TPF-MPF and TPF-MPF/P films. This again correlates with the morphology of the film systems, i.e. films with more porous morphologies are less stable in acidic or alkaline solutions. However, all the film systems had disintegrated by day 24 of immersion in the alkaline medium.

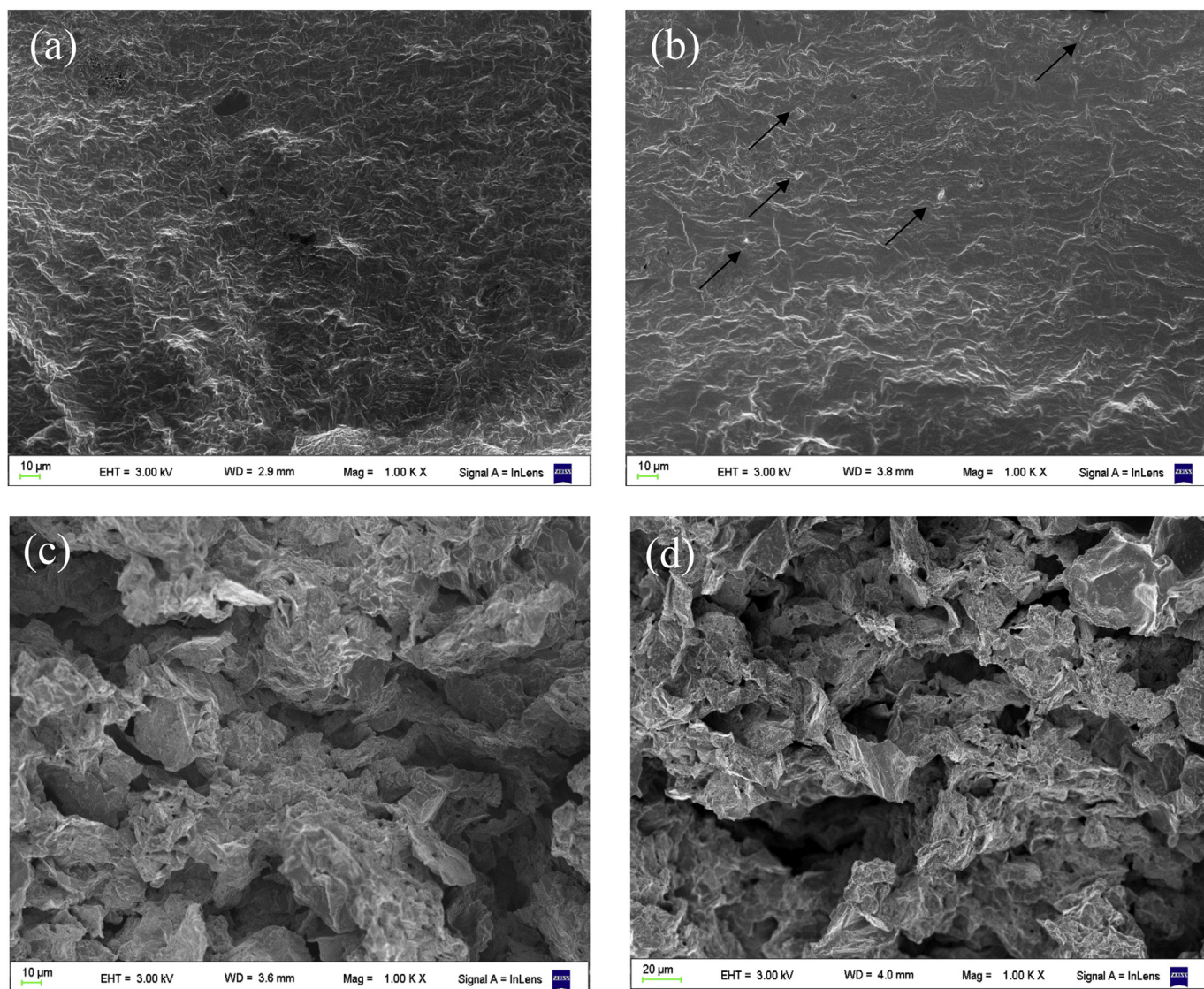


Fig. 7. FESEM micrographs of the cryogenic fracture surface of the films based on: (a) phosphated pumpkin flour (TPF-PPF), (b) phosphated pumpkin flour/plum flour (TPF-PPF/P), (c) methylated pumpkin flour (TPF-MPF) and (d) methylated pumpkin flour/plum flour (TPF-MPF/P). At 1.0 k \times of magnification.

Table 3

Parameters of the uniaxial tensile tests: Young's modulus (E), maximum stress (σ_m), strain at break (ϵ_b) and toughness (T).

Materials	E (MPa)	σ_m (MPa)	ϵ_b (%)	T ($\times 10^5$) (J/m 3)
TPF-PPF	1.0 ± 0.2^a	0.22 ± 0.03^a	27 ± 3^a	0.04 ± 0.10^a
TPF-PPF/P	2.0 ± 0.1^b	0.58 ± 0.02^b	54 ± 3^b	0.55 ± 0.10^b
TPF-MPF	N.d.	N.d.	N.d.	N.d.
TPF-MPF/P	N.d.	N.d.	N.d.	N.d.

Equal letters in the same column indicate no statistically significant difference ($p \leq 0.05$).

Film systems based on: phosphated pumpkin flour (TPF-PPF), phosphated pumpkin flour/plum flour (TPF-PPF/P), methylated pumpkin flour (TPF-MPF) and methylated pumpkin flour/plum flour (TPF-MPF/P).

N.d. = Not determined.

Based on these results, we consider that the phosphated pumpkin flour-based film systems studied (TPF-PPF and TPF-PPF/P) could be applied to slightly acidic foods, since these systems are more stable under these conditions than the methylated systems (TPF-MPF and TPF-MPF/P).

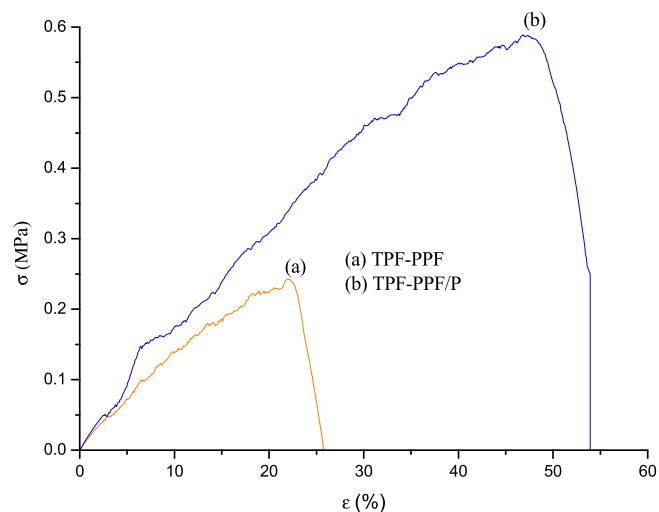


Fig. 8. Stress (σ) – strain (ϵ) curves of the films based on: (a) phosphated pumpkin flour (TPF-PPF) and (b) phosphated pumpkin flour/plum flour (TPF-PPF/P).

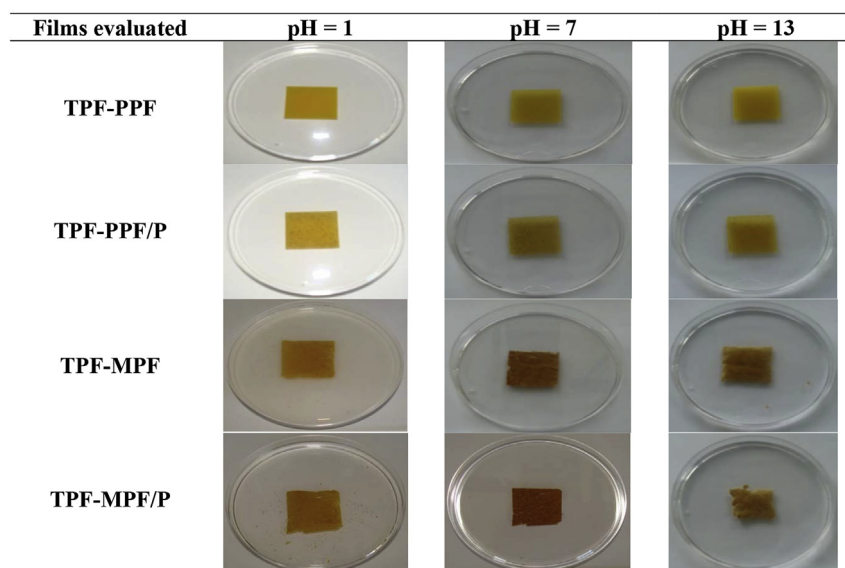


Fig. 9. Response at different pH conditions of the films studied based on: phosphated pumpkin flour (TPF-PPF), phosphated pumpkin flour/plum flour (TPF-PPF/P), methylated pumpkin flour (TPF-MPF) and methylated pumpkin flour/plum flour (TPF-MPF/P).

3.2.8. Biodegradability in vegetable compost & in vivo digestibility tests as an ecotoxicity bioassay

According to [ISO 14855 \(2005, 2007\)](#) any material is considered biodegradable if after six months under compost conditions at 58 °C its initial mass decreases by 90%, whereas the [ASTM D5338 \(2003\)](#) standard requires a 60% reduction in initial mass for homopolymers, and 90% for polymer blends within 180 days. In addition, at least 10% of

the original dry weight of the material should be able to pass through a 2 mm sieve after twelve weeks under compost conditions ([EN 13432, 2000](#); [EN 14995, 2006](#)). Taking into consideration the aforementioned official concepts of biodegradation, the results in this study showed that all the films developed were biodegradable. In fact, they had all completely biodegraded by the second day of the “biodegradability in vegetable compost” test without observing significant differences in the

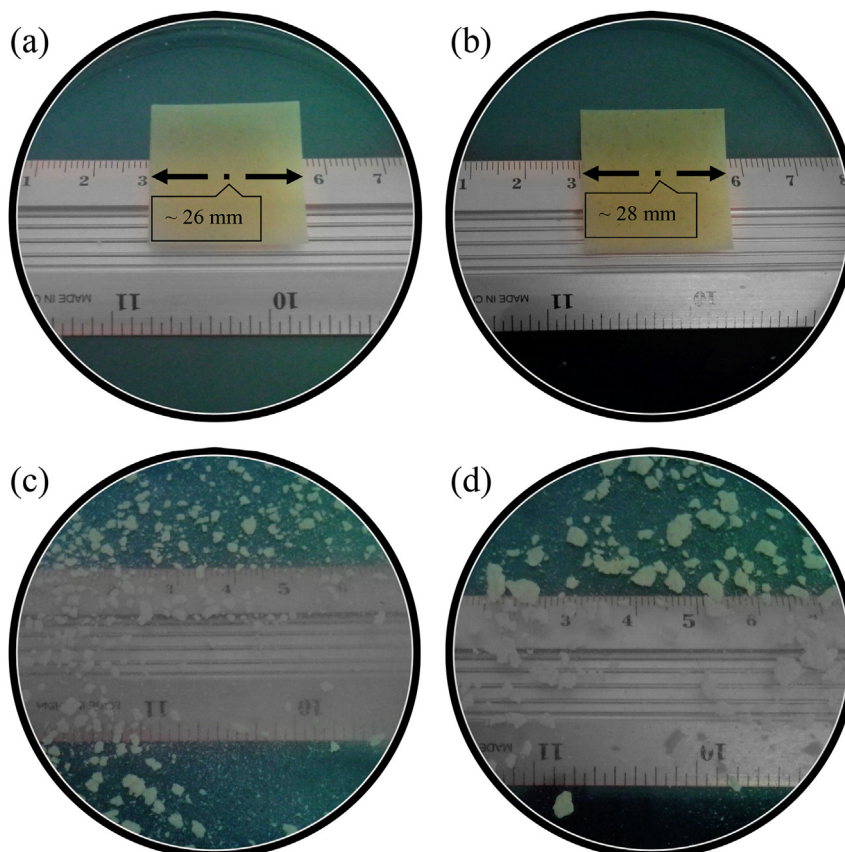


Fig. 10. Digital photographs of the thermoplastic flour (TPF) films immersed in acid medium after 24 days: (a) phosphated pumpkin flour (TPF-PPF), (b) phosphated pumpkin flour/plum flour (TPF-PPF/P), (c) methylated pumpkin flour (TPF-MPF) and (d) methylated pumpkin flour/plum flour (TPF-MPF/P).

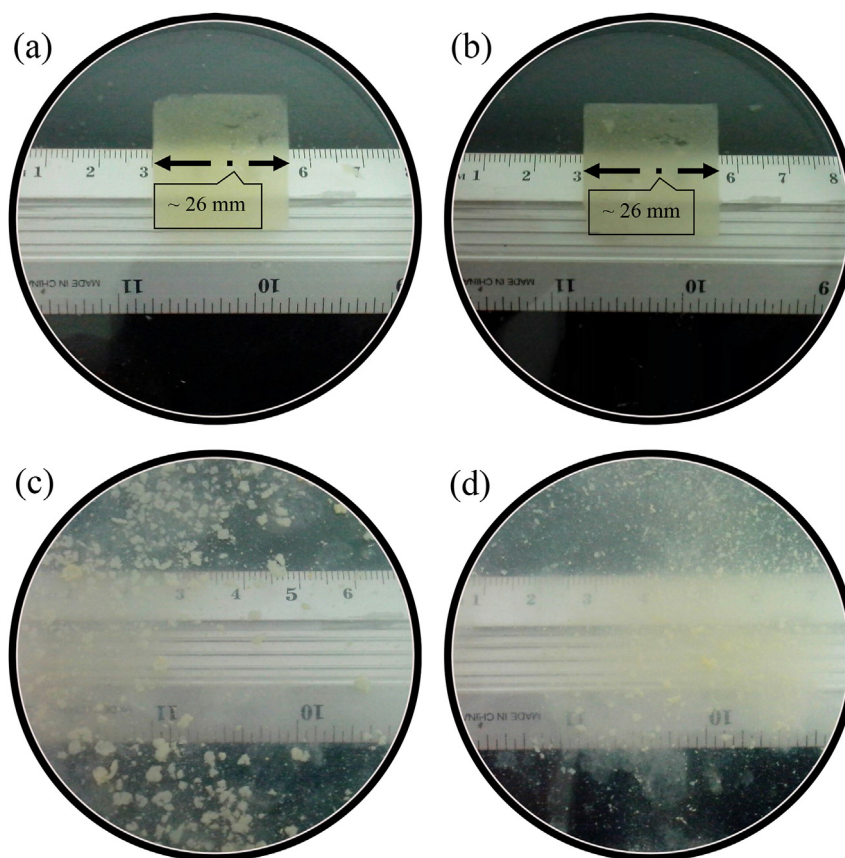


Fig. 11. Digital photographs of the thermoplastic flour (TPF) films immersed in alkaline medium after 17 days: (a) phosphated pumpkin flour (TPF-PPF), (b) phosphated pumpkin flour/plum flour (TPF-PPF/P), (c) methylated pumpkin flour (TPF-MPF) and (d) methylated pumpkin flour/plum flour (TPF-MPF/P).

rate of biodegradation between the two modified film systems (methylated and phosphated) or between films with or without the plum flour nanocomposite, i.e. all the films were 100% biodegradable. These materials were also more biodegradable than other films developed by our research group (Medina Jaramillo et al., 2016), for example, cassava starch-based films containing different concentrations of *yerba mate* (*Ilex paraguariensis*) extract (Medina Jaramillo et al., 2016) where the complete biodegradation of these films was observed after 12 days of being subjected to the biodegradability in vegetable compost test.

The biodegradability of these types of materials is, in fact, well known. There is a false belief, however, that biopolymeric materials, particularly those of natural origin, do not constitute a danger to the environment, i.e. the belief that all biodegradable materials are eco-friendly. Thus, in order to determine whether or not the developed materials were completely eco-friendly we decided to carry out compostability studies, which do assess ecotoxicity. According to ASTM D6400 (2004), the evaluation of the compostability of polymer materials in terms of their ecotoxicity is mainly based on the use of plants, soil fauna (earthworms), aquatic fauna (*Daphnia*, algae (green algae) or microbes (luminescent bacteria). For example, survival and weight changes in compost worms (*Eisenia foetida*) after consuming plastic materials have been used as biomarkers to assess their compostability (ASTM D6400; 2004). In this study, we employed the furniture weevil (*Tricorynus* sp, Coleoptera: Anobiidae) to determine the ecotoxicity of the biopolymeric materials developed. The first relevant result obtained was that the methylated pumpkin flour-based films (TPF-MPF and TPF-MPF/P) caused 100% mortality (0% survival, Fig. 12) of the individuals on day two of the compostability test as opposed to the phosphated pumpkin flour-based films (TPF-PPF and TPF-PPF/P) which only produced a 10% mortality rate (90% survival) over the whole trial period (8 days). These results suggest that methylated pumpkin flour-based

films (TPF-MPF and TPF-MPF/P) are highly ecotoxic (non-edible), i.e. these materials are biodegradable but not compostable. This means that modification by methylation does not lead to the production of compostable, i.e. eco-friendly, plastic materials, whereas modification by phosphating does. This also highlights the fact that not all biodegradable materials are necessarily eco-friendly. It is also worth noting that the recorded mortality rate of furniture weevils fed with the methylated pumpkin flour-based films (TPF-MPF and TPF-MPF/P) may not only be caused by the modified flour itself, but also by BaSO_4 , which is an undesirable by-product of the methylation reaction. Therefore, either altogether or separately one of the two cause total mortality (100%) in the insects fed with the TPF-MPF and TPF-MPF/P films.

As expected from the results described above, the weight changes of the furniture weevils that consumed the TPF-MPF and TPF-MPF/P films were equal to zero. In contrast, the weevils that consumed the TPF-PPF and TPF-PPF/P films showed weight increases of 11% and 23%, respectively, by the end of the trial (8 days). It can thus be said that the incorporation of the nanocomposite in the phosphated film improved its compostability.

4. Conclusions

The phosphated pumpkin flour films were biodegradable and compostable. In contrast, the methylated pumpkin flour films were biodegradable but not compostable due to their ecotoxicity. Thus the phosphated films are eco-friendly, whereas the methylated films, although biodegradable, are not. In addition, the phosphated films had a more compact morphology giving materials that 1) were relatively stable in both acidic and alkaline media, 2) showed a more plastic behavior (low glass transition temperature (T_g) values), and 3) had improved mechanical properties. The methylated films, on the other

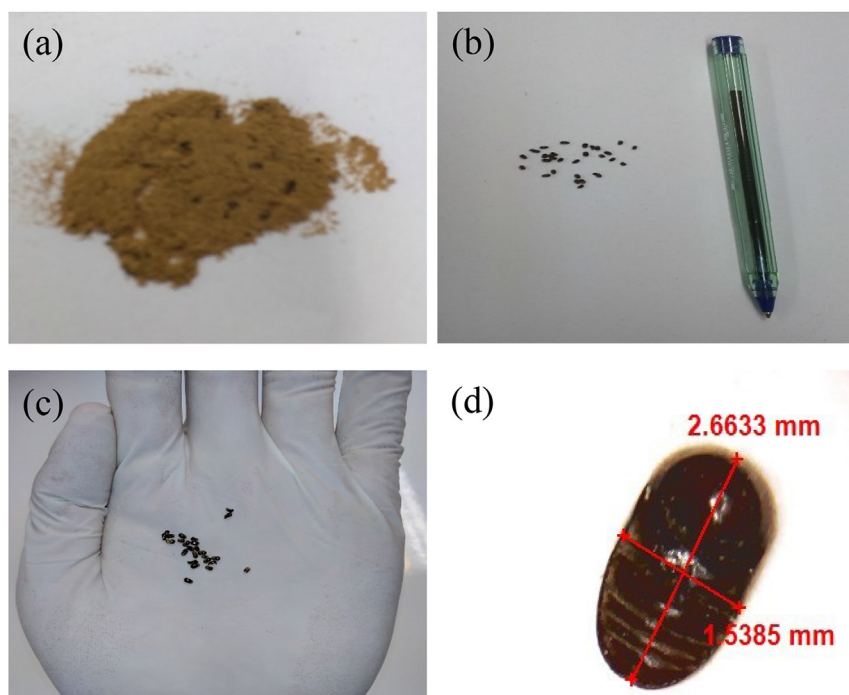


Fig. 12. Compostability study using a bioassay to evaluate the ecotoxicity of films made from methylated pumpkin flour (TPF-MPF and TPF-MPF/P) using the furniture weevil (*Tricorynus* sp, Coleoptera: Anobiidae). **Panel a-** Dead weevils inside the film matrix based on dehydrated, pulverized and sieved methylated pumpkin flour. **Panel b-** Size ratio of the dead weevils used as compared to a ballpoint pen. **Panel c-** Appearance of dead weevils. **Panel d-** Optical micrograph of dead furniture weevils. Film systems based on: methylated pumpkin flour (TPF-MPF) and methylated pumpkin flour/plum flour (TPF-MPF/P).

hand, were less sensitive to moisture and had a higher thermal resistance. However, their brittleness limits their potential applications. We hoped that incorporating the plum flour nanocomposite would lead to the development of pH-sensitive materials due to the anthocyanins contained in the fruit. Unfortunately, however, this goal was not achieved. Nevertheless, the addition of the nanocomposite improved the mechanical properties, as well as increasing film swelling, the T_g values, crystallinity percentage, water contact angle values, and the thermal resistance. It also improved the compostability of these hydrocolloid-based bioplastic materials as measured by the ecotoxicity biomarkers employed.

Conflicts of interest

The author declares no conflict of interest.

Acknowledgements

The author would like to thank the Consejo Nacional de Investigaciones Científicas y Técnicas (CONICET) (Postdoctoral fellowship internal PDTs-Resolution 2417), Universidad Nacional de Mar del Plata (UNMDP) for financial support. Also, Dr. Mirian Carmona-Rodríguez for her valuable contribution. I am also very grateful to Dr. Gema González and M.Sc. Antonio Monsalve from the Venezuelan Institute for Scientific Research, for allowing me to carry out the acquisition of AFM images in their laboratory, and to M.Sc. Kevia Álvarez for performing the AFM study. The water contact angles and TGA measurements were obtained at the LPMC laboratory, and I wish to thank Dr. Silvia Goyanes and Dr. Lucía Famá.

References

- AACC. American Association of Cereal Chemists (2003). *Approved methods of analysis*. Retrieved from: <http://methods.aacnet.org/toc.aspx>.
- Álvarez, K., Álvarez, V. A., & Gutiérrez, T. J. (2018). Biopolymer composite materials with antimicrobial effects applied to the food industry. In V. K. Thakur, & M. K. Thakur (Eds.). *Functional biopolymers* (pp. 57–96). Cham: Springer International Publishing. https://doi.org/10.1007/978-3-319-66417-0_3.
- Álvarez, K., Famá, L., & Gutiérrez, T. J. (2017). Physicochemical, antimicrobial and mechanical properties of thermoplastic materials based on biopolymers with application in the food industry. In M. Masuelli, & D. Renard (Eds.). *Advances in physicochemical properties of biopolymers: Part 1* (pp. 358–400). Bentham Science Publishers. <https://doi.org/10.2174/9781681084534117010015>.
- Amani, N. G., Buléon, A., Kamenan, A., & Colonna, P. (2004). Variability in starch physicochemical and functional properties of yam (*Dioscorea* sp) cultivated in Ivory Coast. *Journal of the Science of Food and Agriculture*, 84(15), 2085–2096. <https://doi.org/10.1002/jsfa.1834>.
- Association of Official Analytical Chemists (AOAC) (1990). *Official methods of analysis*. ASTM D5338-98 (2003). *Standard test method for determining aerobic biodegradation of plastic materials under controlled composting conditions*. Retrieved from: <https://www.astm.org/DATABASE.CART/HISTORICAL/D5338-98R03.htm>.
- ASTM D6400-04 (2004). *Standard specification for compostable plastics*. Retrieved from: <https://www.astm.org/DATABASE.CART/HISTORICAL/D6400-04.htm>.
- Bracone, M., Merino, D., González, J., Álvarez, V. A., & Gutiérrez, T. J. (2016). Nanopackaging from natural fillers and biopolymers for the development of active and intelligent films. In S. Ikram, & S. Ahmed (Eds.). *Natural Polymers: Derivatives, blends and composites* (pp. 119–155). New York: Nova Science Publishers.
- Choi, I., Lee, J. Y., Lacroix, M., & Han, J. (2017). Intelligent pH indicator film composed of agar/potato starch and anthocyanin extracts from purple sweet potato. *Food Chemistry*, 218, 122–128. <https://doi.org/10.1016/j.foodchem.2016.09.050>.
- Condés, M. C., Anón, M. C., Dufresne, A., & Mauri, A. N. (2018). Composite and nanocomposite films based on amaranth biopolymers. *Food Hydrocolloids*, 74, 159–167. <https://doi.org/https://doi.org/10.1016/j.foodhyd.2017.07.013>.
- Deetae, P., Shobsngob, S., Varayanond, W., Chinachoti, P., Naivikul, O., & Varavinit, S. (2008). Preparation, pasting properties and freeze-thaw stability of dual modified crosslink-phosphorylated rice starch. *Carbohydrate Polymers*, 73(2), 351–358. <https://doi.org/https://doi.org/10.1016/j.carbpol.2007.12.004>.
- EN 13432 (2000). *Packaging - requirements for packaging recoverable through composting and biodegradation - test scheme and evaluation criteria for the final acceptance of packaging*. Retrieved from: <https://www.en-standard.eu/csn-en-13432-packaging-requirements-for-packaging-recoverable-through-composting-and-biodegradation-test-scheme-and-evaluation-criteria-for-the-final-acceptance-of-packaging/>.
- EN 14995 (2006). *Plastics - evaluation of compostability - test scheme and specifications*. Retrieved from: <https://www.en-standard.eu/csn-en-14995-plastics-evaluation-of-compostability-test-scheme-and-specifications/>.
- FDA (2017). *CFR - code of federal regulations title 21*. Retrieved from: <https://www.accessdata.fda.gov/scripts/cdrh/cfdocs/cfhr/CFRSearch.cfm?fr=172.892>.
- Ferreira de Almeida, C. L., Alves Brito, S., Italo de Santana, T., Alves Costa, H. B., Reis de Carvalho Júnior, C. H., da Silva, M. V., ... Gonçalves da Silva, T. (2017). *Spondias purpurea* L. (Anacardiaceae): Antioxidant and antitumor activities of the leaf hexane extract. *Oxidative Medicine and Cellular Longevity*, 1–14. <https://doi.org/https://doi.org/10.1155/2017/6593073>.
- Food and Agriculture Organization of the United Nations (FAO) (2007). *Guía técnica para producción y análisis de almidón de yuca*. Retrieved from: <http://www.fao.org/docrep/010/a1028s/a1028s00.htm>.
- Food and Agriculture Organization of the United Nations (FAO). FAO Regional Office for Latin America and the Caribbean (1985). *Insectos que dañan granos productos almacenados*. Santiago de Chile. Retrieved from: <http://www.fao.org/docrep/x5053s/x5053s04.htm#3> Principales órdenes y especies de insectos.
- Food and Agriculture Organization of the United Nations (FAO). FAO Regional Office for Latin America and the Caribbean (2014). *FAO statistical yearbook 2014. Food and agriculture in Latin America and the Caribbean*. Santiago de Chile. Retrieved from:

- <http://www.fao.org/3/a-i3592s.pdf>.
- García-Tejada, Y. V., López-González, C., Pérez-Orozco, J. P., Rendón-Villalobos, R., Jiménez-Pérez, A., Flores-Huicochea, E., ... Bastida, C. A. (2013). Physicochemical and mechanical properties of extruded laminates from native and oxidized banana starch during storage. *LWT - Food Science and Technology*, 54(2), 447–455. <https://doi.org/10.1016/j.lwt.2013.05.041>.
- Gutiérrez, T. J. (2018a). Active and intelligent films made from starchy sources/blackberry pulp. *Journal of Polymers and the Environment*. <https://doi.org/10.1007/s10924-017-1134-y>.
- Gutiérrez, T. J. (2018b). Biodegradability and compostability of food nanopackaging materials. In G. Cirillo, M. A. Kozłowski, & U. G. Spizzirri (Eds.), *Composites materials for food packaging* (pp. 269–296). Wiley. <https://doi.org/10.1002/9781119160243.ch9>.
- Gutiérrez, T. J. (2018c). Plantain flours as potential raw materials for the development of gluten-free functional foods. *Carbohydrate Polymers* (In press).
- Gutiérrez, T. J., & Álvarez, K. (2016). Physico-chemical properties and *in vitro* digestibility of edible films made from plantain flour with added Aloe vera gel. *Journal of Functional Foods*, 26, 750–762. <https://doi.org/10.1016/j.jff.2016.08.054>.
- Gutiérrez, T. J., & Alvarez, V. A. (2017a). Films made by blending poly(ϵ -caprolactone) with starch and flour from sagu rhizome grown at the Venezuelan amazons. *Journal of Polymers and the Environment*, 25(3), 701–716. <https://doi.org/10.1007/s10924-016-0861-9>.
- Gutiérrez, T. J., & Alvarez, V. A. (2017b). Cellulosic materials as natural fillers in starch-containing matrix-based films: A review. *Polymer Bulletin*, 74(6), 2401–2430. <https://doi.org/10.1007/s00289-016-1814-0>.
- Gutiérrez, T. J., & Alvarez, V. A. (2017c). Eco-friendly films prepared from plantain flour/PCL blends under reactive extrusion conditions using zirconium octanoate as a catalyst. *Carbohydrate Polymers*, 178, 260–269. <https://doi.org/10.1016/j.carbpol.2017.09.026>.
- Gutiérrez, T. J., & Alvarez, V. A. (2018). Bionanocomposite films developed from corn starch and natural and modified nano-clays with or without added blueberry extract. *Food Hydrocolloids*. <https://doi.org/10.1016/j.foodhyd.2017.10.017>.
- Gutiérrez, T. J., & González, G. (2016). Effects of exposure to pulsed light on surface and structural properties of edible films made from cassava and taro starch. *Food and Bioprocess Technology*, 9(11), 1812–1824. <https://doi.org/10.1007/s11947-016-1765-3>.
- Gutiérrez, T. J., & González, G. (2017). Effect of cross-linking with Aloe vera gel on surface and physicochemical properties of edible films made from plantain flour. *Food Biophysics*, 12(1), 11–22. <https://doi.org/10.1007/s11483-016-9458-z>.
- Gutiérrez, T. J., González Seligra, P., Medina Jaramillo, C., Famá, L., & Goyanes, S. (2017). Effect of filler properties on the antioxidant response of thermoplastic starch composites. In V. K. Thakur, M. K. Thakur, & M. R. Kessler (Vol. Eds.), *Handbook of composites from renewable materials, structure and chemistry: Vol. 1*, (pp. 337–370). John Wiley & Sons. <https://doi.org/10.1002/9781119441632.ch14>.
- Gutiérrez, T. J., Herniou-Julien, C., Álvarez, K., & Alvarez, V. A. (2018). Structural properties and *in vitro* digestibility of edible and pH-sensitive films made from Guinea arrowroot starch and wastes from wine manufacture. *Carbohydrate Polymers*, 184, 135–143. <https://doi.org/10.1016/j.carbpol.2017.12.039>.
- Gutiérrez, T. J., Morales, N. J., Pérez, E., Tapia, M. S., & Famá, L. (2015). Physico-chemical properties of edible films derived from native and phosphorylated cush-cush yam and cassava starches. *Food Packaging and Shelf Life*, 3, 1–8. <https://doi.org/10.1016/j.fpsl.2014.09.002>.
- Gutiérrez, T. J., Ollier, R., & Alvarez, V. A. (2018). Surface properties of thermoplastic starch materials reinforced with natural fillers. In V. K. Thakur, & M. K. Thakur (Eds.), *Functional biopolymers* (pp. 131–158). Springer International Publishing. https://doi.org/10.1007/978-3-319-66417-0_5.
- Gutiérrez, T. J., Suniaga, J., Monsalve, A., & García, N. L. (2016). Influence of beet flour on the relationship surface-properties of edible and intelligent films made from native and modified plantain flour. *Food Hydrocolloids*, 54, 234–244. <https://doi.org/10.1016/j.foodhyd.2015.10.012>.
- Gutiérrez, T. J., Tapia, M. S., Pérez, E., & Famá, L. (2015). Edible films based on native and phosphorylated 80:20 waxy:normal corn starch. *Starch - Stärke*, 67(1–2), 90–97. <https://doi.org/10.1002/star.201400164>.
- Hassimotto, N. M. A., Mota, R. V. da, Cordenunsi, B. R., & Lajolo, F. M. (2008). Physico-chemical characterization and bioactive compounds of blackberry fruits (*Rubus* sp.) grown in Brazil. *Food Science and Technology (Campinas)*, 28(3), 702–708. <https://doi.org/10.1590/S0101-20612008000300029>.
- Hermans, P. H., & Weidinger, A. (1961). On the determination of the crystalline fraction of polyethylenes from X-ray diffraction. *Macromolecular Chemistry and Physics*, 44(1), 24–36. <https://doi.org/10.1002/macp.1961.020440103>.
- ISO 14855-1:2005 (2005). *Determination of the ultimate aerobic biodegradability of plastic materials under controlled composting conditions – method by analysis of evolved carbon dioxide – Part 1: General method*. Retrieved from: <https://www.iso.org/standard/42155.html>.
- ISO 14855-2:2007 (2007). *Determination of the ultimate aerobic biodegradability of plastic materials under controlled composting conditions – method by analysis of evolved carbon dioxide – Part 2: Gravimetric measurement of carbon dioxide evolved in a laboratory-scale test*. Retrieved from: <https://www.iso.org/standard/40617.html>.
- ISO 527-2 (2012). *Determination of tensile properties of plastics*. Retrieved from: <https://www.iso.org/obp/ui/#iso:std:56046:en>.
- Jay, J. M. (1995). Intrinsic and extrinsic parameters of foods that affect microbial growth. In J. M. Jay (Ed.), *Modern food microbiology* Boston, MA: Springer US. Fifth, pp. 38–66. https://doi.org/10.1007/978-1-4615-7476-7_3.
- Kerr, R., & Cleveland, F. C. (1959). *Orthophosphate esters of starch*. Google Patents.
- Liu, B., Xu, H., Zhao, H., Liu, W., Zhao, L., & Li, Y. (2017). Preparation and characterization of intelligent starch/PVA films for simultaneous colorimetric indication and antimicrobial activity for food packaging applications. *Carbohydrate Polymers*, 157, 842–849. <https://doi.org/10.1016/j.carbpol.2016.10.067>.
- Lovera, M., Pérez, E., & Laurentin, A. (2017). Digestibility of starches isolated from stem and root tubers of arracacha, cassava, cush-cush yam, potato and taro. *Carbohydrate Polymers*, 176, 50–55. <https://doi.org/10.1016/j.carbpol.2017.08.049>.
- Luchese, C. L., Frick, J. M., Patzer, V. L., Spada, J. C., & Tessaro, I. C. (2015). Synthesis and characterization of biofilms using native and modified pinhão starch. *Food Hydrocolloids*, 45, 203–210. <https://doi.org/10.1016/j.foodhyd.2014.11.015>.
- Luchese, C. L., Garrido, T., Spada, J. C., Tessaro, I. C., & de la Caba, K. (2018). Development and characterization of cassava starch films incorporated with blueberry pomace. *International Journal of Biological Macromolecules*, 106, 834–839. <https://doi.org/https://doi.org/10.1016/j.ijbiomac.2017.08.083>.
- Ma, Q., & Wang, L. (2016). Preparation of a visual pH-sensing film based on tara gum incorporating cellulose and extracts from grape skins. *Sensors and Actuators B: Chemical*, 235, 401–407. <https://doi.org/10.1016/j.snb.2016.05.107>.
- Medina Jaramillo, C., Gutiérrez, T. J., Goyanes, S., Bernal, C., & Famá, L. (2016). Biodegradability and plasticizing effect of yerba mate extract on cassava starch edible films. *Carbohydrate Polymers*, 151, 150–159. <https://doi.org/10.1016/j.carbpol.2016.05.025>.
- Mestres, C., Matencio, F., Pons, B., Yajid, M., & Flidel, G. (1996). A rapid method for the determination of amylose content by using differential-scanning calorimetry. *Starch - Stärke*, 48(1), 2–6. <https://doi.org/10.1002/star.19960480103>.
- Muñoz-López, C., Urrea-García, G. R., Jiménez-Fernández, M., Rodríguez-Jiménez, G., del, C., & Luna-Solano, G. (2018). Effect of drying methods on the physicochemical and thermal properties of Mexican plum (*Spondias purpurea* L.). *CyTA - Journal of Food*, 16(1), 127–134. <https://doi.org/10.1080/19476337.2017.1345984>.
- Otoni, C. G., Avena-Bustillos, R. J., Azeredo, H. M. C., Lorevice, M. V., Moura, M. R., Mattoso, L. H. C., et al. (2017). Recent advances on edible films based on fruits and vegetables—a review. *Comprehensive Reviews in Food Science and Food Safety*, 16(5), 1151–1169. <https://doi.org/10.1111/1541-4337.12281>.
- Pacheco, E. (2001). Evaluación nutricional de soppas deshidratadas a base de harina de plátano verde. Digestibilidad *in vitro* de almidón. *Acta Científica Venezolana*, 52(4), 278–282. Retrieved from: <http://acta.ivic.gov.ve/52-4/articulo6.pdf>.
- Pelissari, F. M., Andrade-Mahecha, M. M., Sobral, P. J. do A., & Menegalli, F. C. (2013). Comparative study on the properties of flour and starch films of plantain bananas (*Musa paradisiaca*). *Food Hydrocolloids*, 30(2), 681–690. <https://doi.org/10.1016/j.foodhyd.2012.08.007>.
- Pereira, V. A., de Arruda, I. N. Q., & Stefani, R. (2015). Active chitosan/PVA films with anthocyanins from *Brassica oleraceae* (Red Cabbage) as time-temperature indicators for application in intelligent food packaging. *Food Hydrocolloids*, 43, 180–188. <https://doi.org/10.1016/j.foodhyd.2014.05.014>.
- Popović, S., Peričin, D., Vaštag, Ž., Lazić, V., & Popović, L. (2012). Pumpkin oil cake protein isolate films as potential gas barrier coating. *Journal of Food Engineering*, 110(3), 374–379. <https://doi.org/https://doi.org/10.1016/j.jfoodeng.2011.12.035>.
- Popović, S., Peričin, D., Vaštag, Ž., Popović, L., & Lazić, V. (2011). Evaluation of edible film-forming ability of pumpkin oil cake; effect of pH and temperature. *Food Hydrocolloids*, 25(3), 470–476. <https://doi.org/https://doi.org/10.1016/j.foodhyd.2010.07.022>.
- Prietto, L., Mirapallete, T. C., Pinto, V. Z., Hoffmann, J. F., Vanier, N. L., Lim, L.-T., ... da Rosa Zavareze, E. (2017). pH-sensitive films containing anthocyanins extracted from black bean seed coat and red cabbage. *LWT - Food Science and Technology*, 80, 492–500. <https://doi.org/10.1016/j.lwt.2017.03.006>.
- Ramaswamy, V., Vimalathithan, R. M., & Ponnusamy, V. (2010). Synthesis and characterization of BaSO₄ nano particles using micro emulsion technique. *Advances in Applied Science Research*, 1(3), 197–204.
- Sengupta, T., & Han, J. H. (2014). Surface chemistry of food, packaging, and biopolymer materials. In J. H. Han (Ed.), *Innovations in food packaging* (pp. 51–86). (2nd ed.). San Diego: Academic Press. <https://doi.org/https://doi.org/10.1016/B978-0-12-394601-0.00047-7>.
- Sivoli, L., Pérez, E., Caraballo, D., Rodríguez, J. P., Rodríguez, D., Moret, J., ... Alvarez-Barreto, J. F. (2013). Cytocompatibility of a matrix of methylated cassava starch and chitosan. *Journal of Cellular Plastics*, 49(6), 507–520. <https://doi.org/10.1177/0021955X13503843>.
- Van Soest, P. U., & Wine, R. H. (1967). Use of detergents in the analysis of fibrous feeds. IV. Determination of plant cell-wall constituents. *Journal of the Association Official of Analytical Chemistry*, 50(1), 50–55.
- Yoshida, C. M. P., Maciel, V. B. V., Mendonça, M. E. D., & Franco, T. T. (2014). Chitosan biobased and intelligent films: Monitoring pH variations. *LWT - Food Science and Technology*, 55(1), 83–89. <https://doi.org/10.1016/j.lwt.2013.09.015>.
- Zeppa, C., Gouanvé, F., & Espuche, E. (2009). Effect of a plasticizer on the structure of biodegradable starch/clay nanocomposites: Thermal, water-sorption, and oxygen-barrier properties. *Journal of Applied Polymer Science*, 112(4), 2044–2056. <https://doi.org/10.1002/app.29588>.